Science
AAAS

Orbital and Millennial Antarctic Climate Variability over the Past 800,000 Years
J. Jouzel, *et al.*
Science **317**, 793 (2007);
DOI: 10.1126/science.1141038

Orbital and Millennial Antarctic Climate Variability over the Past 800,000 Years

J. Jouzel,[1]* V. Masson-Delmotte,[1] O. Cattani,[1] G. Dreyfus,[1] S. Falourd,[1] G. Hoffmann,[1] B. Minster,[1] J. Nouet,[1] J. M. Barnola,[2] J. Chappellaz,[2] H. Fischer,[3] J. C. Gallet,[2] S. Johnsen,[4,5] M. Leuenberger,[6] L. Loulergue,[2] D. Luethi,[6] H. Oerter,[3] F. Parrenin,[2] G. Raisbeck,[7] D. Raynaud,[2] A. Schilt,[6] J. Schwander,[6] E. Selmo,[8] R. Souchez,[9] R. Spahni,[6] B. Stauffer,[6] J. P. Steffensen,[2] B. Stenni,[10] T. F. Stocker,[6] J. L. Tison,[9] M. Werner,[11] E. W. Wolff[12]

A high-resolution deuterium profile is now available along the entire European Project for Ice Coring in Antarctica Dome C ice core, extending this climate record back to marine isotope stage 20.2, ~800,000 years ago. Experiments performed with an atmospheric general circulation model including water isotopes support its temperature interpretation. We assessed the general correspondence between Dansgaard-Oeschger events and their smoothed Antarctic counterparts for this Dome C record, which reveals the presence of such features with similar amplitudes during previous glacial periods. We suggest that the interplay between obliquity and precession accounts for the variable intensity of interglacial periods in ice core records.

The European Project for Ice Coring in Antarctica (EPICA) has provided two deep ice cores in East Antarctica, one (EDC) at Dome C (*1*), on which we focus here, and one (EDML) in the Dronning Maud Land area (*2*). The Dome C drilling [fig. S1 and supporting online material (SOM) text] was stopped at a depth of 3260 m, about 15 m above the bedrock. A preliminary low-resolution δD record was previously obtained from the surface down to 3139 m with an estimated age at this depth of 740,000 years before the present (740 ky B.P.), corresponding to marine isotope stage (MIS) 18.2 (*1*). Other data, such as grain radius, dust concentration, dielectric profile, and electrical conductivity, as well as chemical data (*3*), are available down to this depth, and analyses of the entrapped air have extended the greenhouse gas record—i.e., CO_2, CH_4, and N_2O—back to MIS 16, ~650 ky B.P. (*4*, *5*).

We completed the deuterium measurements, δD_{ice}, at detailed resolution from the surface down to 3259.7 m. This new data set benefits from a more accurate dating and temperature calibration of isotopic changes based on a series of recent simulations performed with an up-to-date isotopic model. In turn, this very detailed Antarctic surface temperature record sheds light on climate analyses in four ways: (i) It allows reliable extension of the climate record back to MIS 20.2 (~800 ky B.P.); (ii) it resolves Antarctic millennial variability over eight successive glacial periods; (iii) it allows quantifiable comparison of the strengths of the successive interglacial and glacial periods; and (iv) the improved time scale allows more accurate investigation of the links between Antarctic temperature and orbital forcing.

This detailed and continuous δD_{ice} profile is shown as a function of time in Fig. 1 and on a depth scale in figs. S2 and S3. For our analysis, we adopted a more precise time scale (SOM text), in which EDC3 has a precision of ±5 ky on absolute ages and of ±20% for the duration of events (*6*, *7*). This scale clearly indicates that the Antarctic counterpart of MIS 15.1 was too long by about a factor 2 in EDC2 (*1*), as already suggested from the comparison with the deep-sea core record (*8*), whereas the scale confirms the long duration of MIS 11.3 (*1*).

The deep-sea benthic oxygen-18 record (*8*) and the δD_{ice} Dome C record are in excellent overall agreement back to ~800 ky B.P. (MIS 20.2), which suggests that our extended EPICA Dome C record now entirely encompasses glacial stage MIS 18 and interglacial MIS 19. This agreement does not hold true for the earlier part of the record below ~3200 m, and we have strong arguments that the core stratigraphy has been disturbed over its bottom 60 m (SOM text). In contrast, the stratigraphic continuity of the record above ~3200 m is supported by all available data, including preliminary CO_2 and CH_4 measurements performed along the transition between MIS 20.2 and 19 (SOM text). We are thus confident that the Dome C δD record provides an ~800-ky-old reliable climatic record.

Results derived from a series of experiments performed with the European Centre/Hamburg Model General Circulation Model implemented with water isotopes (*9*) for different climate stages (SOM text) allowed us to assess the validity of the conventional interpretation of ice core isotope profiles (δD or $\delta^{18}O$) from inland Antarctica, in terms of surface temperature shifts (fig. S4). We inferred that the change in surface temperature (ΔT_s) range, based on 100-year mean values, was ~15°C over the past 800 ky, from –10.3°C for the coldest 100-year interval of MIS 2 to +4.5°C for the warmest of MIS 5.5 (Fig. 2). Despite some differences, the three long East Antarctic isotopic records, Dome C, Vostok (*10*, *11*), and Dome F (*12*), show a very high level of similarity over their common part and the EDC temperature record is expected to be representative of East Antarctica. All glacial stages before 430 ky B.P. are warmer than MIS 2, by ~1°C for MIS 12, 16 and 18 and by ~2°C for MIS 14 (Fig. 2).

We confirm that the early interglacial periods, now including MIS 19, were characterized by less pronounced warmth than those of the past four climatic cycles (*1*). Whereas peak temperatures in the warm interglacials of the later part of the record (MIS 5.5, 7.5, 9.3, and 11.3) were 2° to 4.5°C higher than the last millennium, maximum temperatures were ~1° to 1.5°C colder for MIS 13, 15.1, 15.5, and 17, reaching levels typical of interstadials, such as 7.1 and 7.3. MIS 19 shows the warmest temperature for the period before T_v (~ –0.5°C). For MIS 11 to MIS 17, with the exception of MIS 15.1, peak warmth occurred at the end of the warm periods in contrast with the more recent interglacials for which earlier peak warmth was typical (Fig. 2).

Although isotopic records from Antarctica do not exhibit the rapid and large climate variability observed in Greenland records for the so-called Dansgaard-Oeschger (DO) events of the last glacial period (*13*–*15*), they clearly exhibit millennial-scale variability with muted and more symmetrical events. Synchronization based on gas indicators unambiguously showed that large DO events have Antarctic counterparts (*16*, *17*), and there were indications that shorter events also have such counterparts both from Vostok and Dome C cores (*18*–*20*).

The recent high-resolution EDML isotopic profile over the last glacial period has unambiguously revealed a one-to-one correspondence between all these Antarctic Isotope Maxima (AIM) and DO events (*2*), which with a few exceptions holds true for the EDC core over the entire last glacial period back to DO 25 (Fig. 2 and fig. S5). At Dome C, the typical amplitude of larger events is ~2°C, much lower than for corresponding DO warmings in Greenland, which are often larger than 8°C and as high as 16°C (*21*, *22*).

[1]Laboratoire des Sciences du Climat et l'Environnement/Institut Pierre Simon Laplace, CEA-CNRS–Université de Versailles Saint-Quentin en Yvelines, CE Saclay, 91191, Gif-sur-Yvette, France. [2]Laboratoire de Glaciologie et Géophysique de l'Environnement, CNRS/Université Joseph Fourier, Boîte Postale 96, 38402, Saint Martin d'Hères, France. [3]Alfred Wegener Institute for Polar and Marine Research, Columbusstrasse, D27568 Bremerhaven, Germany. [4]Department of Geophysics, Juliane Maries Vej 30, University of Copenhagen, DK-2100, Copenhagen, Denmark. [5]Science Institute, University of Reykjavik, Dunhaga 3, Reykjavik 107, Iceland. [6]Physics Institute, University of Bern, Sidlerstrasse 5, CH-3012 Bern, Switzerland. [7]Centre de Spectrométrie Nucléaire et de Spectrométrie de Masse/CNRS, Bat 108, 91405, Orsay, France. [8]Department of Earth Sciences, University of Parma, 43100 Parma, Italy. [9]Département des Sciences de la Terre et de l'Environnement, Université Libre de Bruxelles, Brussels, Belgium. [10]Department of Geological, Environmental and Marine Sciences, University of Trieste, 34127 Trieste, Italy. [11]Max Planck Institute for Biogeochemistry, 100164, D7701 Jena, Germany. [12]British Antarctic Survey, High Cross, Madingley Road, Cambridge, CB3 0ET, UK.

*To whom correspondence should be addressed. E-mail: jean.jouzel@lsce.ipsl.fr

Although some AIM events are more prominent in one of the two EPICA sites (fig. S5), they record millennial variability of comparable magnitude (SOM text), despite the fact that EDML is situated in the Atlantic sector whereas Dome C is facing the Indo-Pacific Ocean. Atmospheric circulation and/or efficient circumpolar oceanic currents can contribute to distribute such climatic signals around Antarctica. This detailed comparison between EDC and EDML records further supports the thermal bipolar seesaw hypothesis (*23*), which postulates that abrupt shutdowns and initiations of the Atlantic meridional overturning circulation produce slow warmings and coolings in the Southern Ocean and Antarctic region.

Our record exhibits quite similar millennial climate variability during the past three glacial periods, in terms of both magnitude and pacing (fig. S5), suggesting this was also the case in the North Atlantic, as indicated by sediment data (*24*) and inferred from CH_4 data from Antarctic cores (*5*, *25*). Our lower temporal resolution prevents clear detection of small AIM for earlier glacials, but the amplitude of large AIM, thus presumably of large DO events, does not appear to be substantially influenced by the smaller extent of Northern Hemisphere ice sheets before Termination V. In particular, a very well featured sequence is displayed by the additional cycle provided by the extension of the core from 740 and 800 ky B.P. (Fig. 2 and fig. S5) with three well-marked oscillations that have not yet had counterparts identified in the MIS 18 ocean record (*8*). Finally, our record shows that during each glacial period, AIM events appear once Antarctic temperatures have dropped by at least 4°C below late Holocene temperature (Fig. 2). We suggest that decreases in Antarctic temperature over glacial inceptions modified the formation of Antarctic bottom waters and that the associated reorganization in deep ocean circulation is the key for the onset of glacial instabilities.

Obliquity changes were previously invoked to explain the change in amplitude between glacial and interglacial periods at the time of the Mid-Brunhes Event (MBE), ~430 ky B.P. (*1*). This key characteristic of the EDC δD record is now fully supported by our 800-ky detailed temperature record and its improved EDC3 time scale (Fig. 3). Dominated by a periodicity of ~100 ky, the power spectra of ΔT_s (fig. S6) also reveal a strong obliquity component and point to the influence of the precession, at least for 0 to 400 ky. The relative strength of the obliquity and 100-ky components increases when going from past to present, which is consistent with the increasing amplitude of obliquity variations over the past 800 ky due to a 1.2-million-year modulation (*26*). The 40-ky component is particularly strong, accounting for one-third (4.3°C) of the total range of temperature in the 800-ky record (Fig. 3). Also noticeable are its strong coherency with 65°N summer insolation in the obliquity range (0.97) and its substantial ~5-ky lag with respect to obliquity (fig. S7).

Intermediate-complexity climate models indeed capture a high-latitude signature in annual mean temperature in response to extreme configurations of obliquity, albeit half of that observed here (*27*). With respect to the strong linear relationship between δD and obliquity, the link may be local insolation changes, which at 75°S vary by ~8% up to 14 W/m^2 (*28*). Such changes in high-latitude insolation may be amplified by associated changes in heat and moisture transport in the atmosphere (including water vapor and sea-ice feedbacks at high latitudes). They can thus generate changes in the density of ocean surface waters and therefore in ocean thermohaline circulation; such processes involve deep ocean heat storage with constants of millennia. Notably, the obliquity components of temperature records from the tropical Pacific and from Antarctica are in phase (*29*) within age scale uncertainties. They are thus in phase with the mean annual insolation at high latitude but out of phase with the obliquity component of the mean annual insolation in the tropics. This indicates that mechanisms transferring the high-latitude effect of obliquity

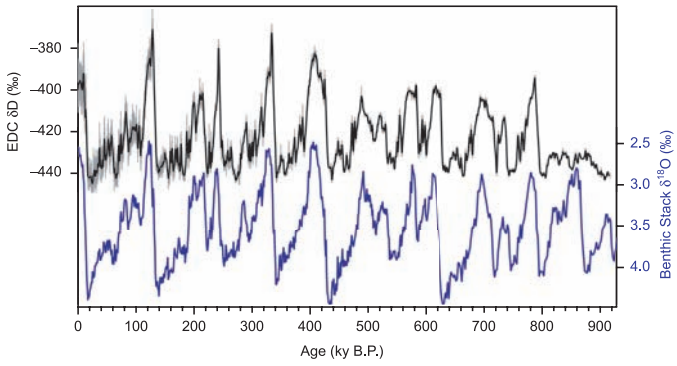

Fig. 1. Comparison of the δD Dome C record on the EDC3 time scale (with all data points in light gray and a smoothed curve in black) with the benthic oxygen-18 record (blue) on its own time scale (*8*). The 3259.7-m δD record, which includes published results down to 788 m (*38*), benefits from an improved accuracy (1σ of ± 0.5‰) and a much more detailed resolution of 55 cm all along the core, whereas the previously published record was based on 3.85-m samples (*1*). The agreement between the two time series back to ~800 ky B.P. justifies the use of oceanic sediment nomenclature (MIS) for describing the ice core record.

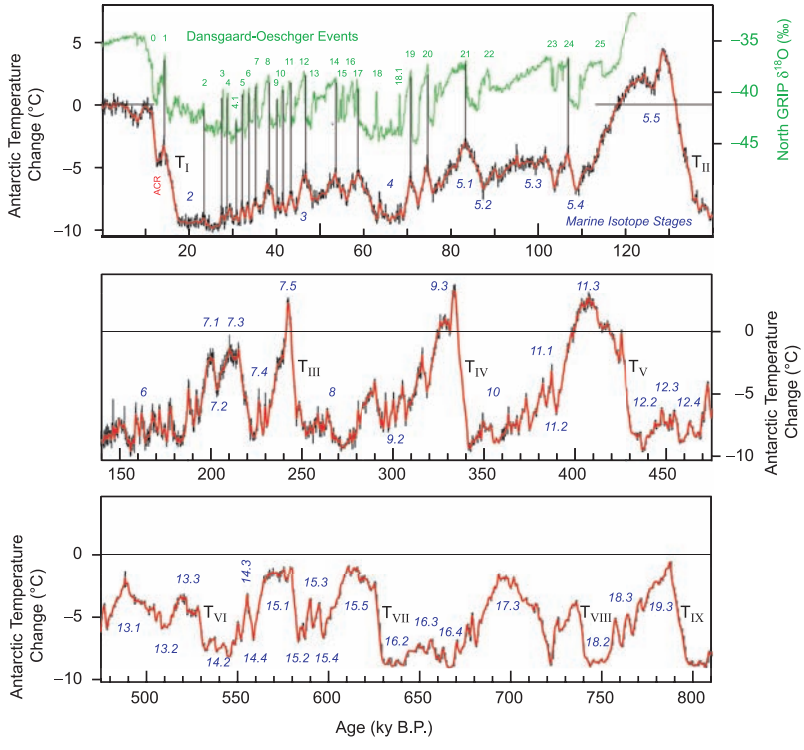

Fig. 2. Dome C temperature anomaly as a function of time over the past 810 ky. Back to 140 ky B.P., we report 100-year mean values, whereas for earlier periods (middle and lower traces), ΔT_s is calculated from 0.55-m raw data; a smooth curve using a 700-year binomial filter is superimposed on this detailed record. In the upper trace (which is plotted on a more highly resolved time axis), we show the correspondence between the DO events as recorded in the North Greenland Ice Core Project isotopic record (*2*, *15*) and AIM events recorded in the EDC temperature record during the last glacial period and the last deglaciation. We have indicated the successive MIS, and the transitions are labeled from T_I to T_{IX}.

toward the tropics may involve changes in heat export from the tropics.

Our EDC ice core shows no indication that greenhouse gases have played a key role in such a coupling. Not only does the obliquity component of the radiative forcing—calculated accounting for both CO_2 and CH_4 changes (*30*)—have a small amplitude over the past 650 ky (~0.5 W/m^2, Fig. 3) but it also seems to lag Antarctic and tropical temperature changes. Nor can this in-phase temperature behavior be explained by local insolation, given that this parameter is in anti-phase between low and high latitudes. Rather than assuming that this is caused by greenhouse coupling, we suggest that it results from a transfer of the high-latitude obliquity signal to the tropics through rapid processes involving atmospheric circulation or intermediate oceanic waters, possibly linked, as documented from present-day climates (*31*) and examined for past climates (*32*), with changes in sea-ice around Antarctica. The amplitude of the radiative greenhouse forcing, however, is very important in the 100-ky band (~2.5 W/m^2 comparable to the additional greenhouse forcing due to anthropogenic activities). This points to a strong carbon-cycle feedback involved in the magnitude and possibly duration of ice ages (*33*) and to a global character of the Antarctic temperature record.

One key question in this frequency band concerns the relative role of the different orbital parameters in driving terminations. Some authors suggest that terminations occur at multiples of obliquity (*34*, *35*) or precession cycles (*36*). The latter includes the insolation canon hypothesis that calls upon the interplay of precession and obliquity with considerations of total energy input and threshold effects (*37*). With our current age scale, the insolation canon approach works well for T_I to T_{IV} but not for earlier terminations. We support the view of combined effects of precession and obliquity in driving ice age dynamics but suggest that the role of obliquity is underestimated by this approach [e.g., high-latitude insolation should not be considered for mid-month but integrated over several months (*35*)].

The strength of interglacials is highly variable along the record. We suggest that this variation results from an interplay between obliquity and precession (Fig. 3). When 65°N summer insolation (or the inverted precession parameter) and obliquity changes peak in phase (within 5 ky), their combined effects induce strong interglacial periods (MIS 1, 5, 9, 11, and 19). When they are in antiphase, compensating effects induce weak interglacial intensities (MIS 13, 15, 17, and 7.3). In this line, we calculated for each interglacial the cumulative warmth defined with respect to a temperature threshold; we then explored the relationship between this index and insolation. This analysis accounts for the effects of both precession (in the timing of glacial-interglacial transitions) and obliquity (through the mean annual high-latitude insolation). The most robust result is obtained when comparing the cumulative warmth with the cumulative high-latitude insolation (above its average value and taking into account the phase lag of 5 ky). Whereas for small changes in insolation, there is no clear relationship between these two, a linear relationship is observed when the cumulative insolation is larger than ~1700 GJ/m^2 (fig. S8). In turn, we suggest a causal link between the change of amplitude observed in the EDC temperature record and the modulated amplitude of obliquity.

Our new high-resolution Antarctic climate record is able to resolve systematic long-term as well as millennial changes over the past 800,000 years. Whereas the former may be controlled by local insolation changes largely induced by the obliquity cycle, the latter are induced by changes in North Atlantic deep water formation through the thermal bipolar seesaw. Clearly shown for the last glacial cycle, this is also suggested for earlier glacial periods. Overall, our Antarctic temperature record points to an active role for high southern latitudes in the dynamics of climate change both at orbital and millennial time scales, rather than to a picture of these polar regions simply recording variability originating from other parts of the climate system. This climate record will now serve as a benchmark for exploiting the many properties that are, or will be in the near future, measured on the Dome C core, both in the ice (elemental and isotopic composition of dust and of chemical compounds) and in the gas phase (records of greenhouse gases, other atmospheric compounds, and their isotopic signatures).

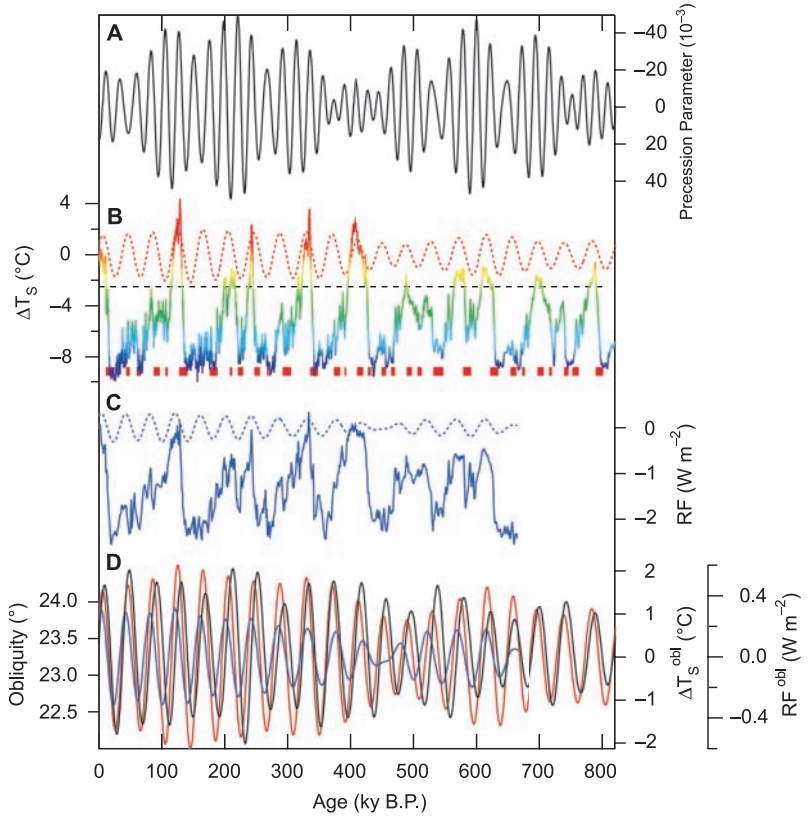

Fig. 3. (**A**) Precession parameter displayed on an inversed vertical axis (black line). (**B**) EDC temperature [solid line, rainbow colors from blue (cold temperatures) to red (warm temperatures)] and its obliquity component extracted using a Gaussian filter within the frequency range 0.043 ± 0.015 ky^{-1} [dashed red line, also displayed in (D) as a solid red line on a different scaling]. Red rectangles indicate periods during which obliquity is increasing and precession parameter is decreasing. (**C**) Combined top-of-atmosphere radiative forcing due to CO_2 and CH_4 (solid blue) and its obliquity component [dashed blue, also displayed in (D) as a solid blue line on a different scaling]. (**D**) Obliquity (solid black line), obliquity component of EDC temperature (red line), and obliquity component of the top-of-atmosphere radiative forcing due to CO_2 and CH_4 (blue). Insolations were calculated using the Analyseries software (*39*).

References and Notes

1. EPICA Community members, *Nature* **429**, 623 (2004).
2. EPICA Community members, *Nature* **444**, 195 (2006).
3. E. W. Wolff *et al.*, *Nature* **440**, 491 (2006).
4. U. Siegenthaler *et al.*, *Science* **310**, 1313 (2005).
5. R. Spahni *et al.*, *Science* **310**, 1317 (2005).
6. F. Parrenin *et al.*, *Clim. Past* **3**, 243 (2007).
7. G. Dreyfus *et al.*, *Clim. Past* **3**, 341 (2007).
8. L. Lisiecki, M. E. Raymo, *Paleoceanography* **20**, PA1003 (2005).
9. G. Hoffmann, M. Werner, M. Heimann, *J. Geophys. Res.* **103**, 16871 (1998).
10. J. R. Petit *et al.*, *Nature* **399**, 429 (1999).
11. D. Raynaud *et al.*, *Nature* **436**, 39 (2005).
12. O. Watanabe *et al.*, *Nature* **422**, 509 (2003).
13. W. Dansgaard *et al.*, *Nature* **364**, 218 (1993).
14. P. M. Grootes, M. Stuiver, J. W. C. White, S. J. Johnsen, J. Jouzel, *Nature* **366**, 552 (1993).

15. North Greenland Ice-core project (NorthGRIP), *Nature* **431**, 147 (2004).
16. T. Blunier, E. J. Brook, *Science* **291**, 109 (2001).
17. N. Caillon *et al.*, *Geophys. Res. Lett.* **30**, 1899 (2003).
18. F. Yiou *et al.*, *J. Geophys. Res.* **102**, 26783 (1997).
19. M. Bender, B. Malaizé, J. Orchado, T. Sowers, J. Jouzel, in *Geophys. Monogr. Am. Geophys. Union 112*, P. U. Clark, R. S. Webb, L. D. Keigwin, Eds. (American Geophysical Union, Washington, DC, 1999), pp. 149–164.
20. B. Stenni *et al.*, *Earth Planet. Sci. Lett.* **217**, 183 (2004).
21. A. Landais, J. Jouzel, V. Masson-Delmotte, N. Caillon, *CRAS* **377**, 947 (2005).
22. C. Huber *et al.*, *Earth Planet. Sci. Lett.* **243**, 504 (2006).
23. T. Stocker, S. J. Johnsen, *Paleoceanography* **18**, 1087 (2003).
24. M. Delmotte *et al.*, *J. Geophys. Res.* **109**, D12104 (2004).
25. J. F. McManus, D. W. Oppo, J. L. Cullen, *Science* **283**, 971 (1999).
26. H. Palike, N. J. Shackleton, U. Rohl, *Earth Planet. Sci. Lett.* **193**, 589 (2001).
27. V. Masson-Delmotte, *Clim. Past* **2**, 145 (2006).
28. A. L. Berger, *J. Atmos. Sci.* **35**, 2362 (1978).
29. M. Medina-Elizalde, D. Lea, *Science* **310**, 1009 (2005).
30. The radiative forcing is calculated using the mathematical formulation described in F. Joos, *PAGES News*, **13**, 11 (2005).
31. X. J. Yuan, D. G. Martinson, *J. Clim.* **13**, 1697 (2000).
32. S. Y. Lee, C. Poulsen, *Earth Planet. Sci. Lett.* **248**, 253 (2006).
33. F. Parrenin, D. Paillard, *Earth Planet. Sci. Lett.* **214**, 243 (2003).
34. P. Huybers, C. Wunsch, *Nature* **434**, 491 (2005).
35. P. Huybers, *Science* **313**, 508 (2006).
36. M. E. Raymo, L. E. Lisiecki, K. H. Nisancioglu, *Science* **313**, 492 (2006).
37. K. G. Schulz, R. E. Zeebe, *Earth Planet. Sci. Lett.* **249**, 326 (2006).
38. J. Jouzel *et al.*, *Geophys. Res. Lett.* **28**, 3199 (2001).
39. D. Paillard, L. Labeyrie, P. Yiou, *Eos Trans. AGU* **77**, 379 (1996).
40. This work is a contribution to EPICA, a joint European Science Foundation/European Commission (EU) scientific program, funded by the EU and by national contributions from Belgium, Denmark, France, Germany, Italy, The Netherlands, Norway, Sweden, Switzerland, and the UK. This is EPICA publication number 181. This work has in particular benefited from the support of EPICA-MIS of the European 6th framework and Agence Nationale de la Recherche (ANR), Integration des Constraintes Paléoclimatiques pour Réduire les Incertitudes sur l'Evolution du Clìmat pendant les Périodes Chaudes (PICC). The main logistic support was provided by Institut Polaire Français Paul-Emile Victor and Programma Nazionale Ricerche in Antartide (at Dome C) and Alfred Wegener Institute (at Dronning Maud Land). We thank the Dome C logistics teams (led by late M. Zucchelli and G. Jugie) and the drilling team that made the science possible. This work has benefited from discussions with H. Pälike.

Supporting Online Material

www.sciencemag.org/cgi/content/full/1141038/DC1
SOM Text
Figs. S1 to S8
References

8 February 2007; accepted 11 June 2007
Published online 5 July 2007;
10.1126/science.1141038
Include this information when citing this paper.

Improved Surface Temperature Prediction for the Coming Decade from a Global Climate Model

Doug M. Smith,* Stephen Cusack, Andrew W. Colman, Chris K. Folland, Glen R. Harris, James M. Murphy

Previous climate model projections of climate change accounted for external forcing from natural and anthropogenic sources but did not attempt to predict internally generated natural variability. We present a new modeling system that predicts both internal variability and externally forced changes and hence forecasts surface temperature with substantially improved skill throughout a decade, both globally and in many regions. Our system predicts that internal variability will partially offset the anthropogenic global warming signal for the next few years. However, climate will continue to warm, with at least half of the years after 2009 predicted to exceed the warmest year currently on record.

It is very likely that the climate will warm over the coming century in response to changes in radiative forcing arising from anthropogenic emissions of greenhouse gases and aerosols (*1*). There is, however, particular interest in the coming decade, which represents a key planning horizon for infrastructure upgrades, insurance, energy policy, and business development. On this time scale, climate could be dominated by internal variability (*2*) arising from unforced natural changes in the climate system such as El Niño, fluctuations in the thermohaline circulation, and anomalies of ocean heat content. This could lead to short-term changes, especially regionally, that are quite different from the mean warming (*3*–*5*) expected over the next century in response to anthropogenic forcing. Idealized studies (*6*–*12*) show that some aspects of internal variability could be predictable several years in advance, but actual predictive skill assessed against real observations has not previously been reported beyond a few seasons (*13*).

Met office Hadley Centre, FitzRoy Road, Exeter, Ex1 3PB, UK.

*To whom correspondence should be addressed. E-mail: doug.smith@metoffice.gov.uk

Global climate models have been used to make predictions of climate change on decadal (*14*, *15*) or longer time scales (*4*, *5*, *16*), but these only accounted for projections of external forcing, neglecting initial condition information needed to predict internal variability. We examined the potential skill of decadal predictions using the newly developed Decadal Climate Prediction System (DePreSys), based on the Hadley Centre Coupled Model, version 3 (HadCM3) (*17*), a dynamical global climate model (GCM). DePreSys (*18*) takes into account the observed state of the atmosphere and ocean in order to predict internal variability, together with plausible changes in anthropogenic sources of greenhouse gases and aerosol concentrations (*19*) and projected changes in solar irradiance and volcanic aerosol (*20*).

We assessed the accuracy of DePreSys in a set of 10-year hindcasts (*21*), starting from the first of March, June, September, and December from 1982 to 2001 (*22*) inclusive (80 start dates in total, although those that project into the future cannot be assessed at all lead times). We also assessed the impact of initial condition information by comparing DePreSys against an additional hindcast set (hereafter referred to as NoAssim), which is identical to DePreSys but does not assimilate the observed state of the atmosphere or ocean. Each NoAssim hindcast consists of four ensemble members, with initial conditions at the same 80 start dates as the DePreSys hindcasts taken from four independent transient integrations (*3*) of HadCM3, which covered the period from 1860 to 2001 (*18*). The NoAssim hindcasts sampled a range of initial states of the atmosphere and ocean that were consistent with the internal variability of HadCM3 but were independent of the observed state. In contrast, the DePreSys hindcasts were initialized by assimilating atmosphere and ocean observations into one of the transient integrations (*18*). In order to sample the effects of error growth arising from imperfect knowledge of the observed state, four DePreSys ensemble members were initialized from consecutive days preceding and including each hindcast start date (*23*). Fig. S1 summarizes our experimental procedure.

We measured the skill of the hindcasts in terms of the root mean square error (RMSE) (*24*) of the ensemble average and tested for differences over our hindcast period between DePreSys and NoAssim that were unlikely to be accounted for by uncertainties arising from a finite ensemble size and a finite number of validation points (*18*). We found that global anomalies (*25*) of annual mean surface temperature (T_s) were predicted with significantly more skill by DePreSys than by NoAssim throughout the range of the hindcasts (compare the solid red curve with the blue shading in Fig. 1A). Averaged over all forecast lead times, the RMSE of global annual mean T_s is 0.132°C for NoAssim as compared with 0.105°C for DePreSys, representing a 20% reduction in RMSE and a 36% reduction in error variance (*E*). Furthermore, the improvement was even greater for multiannual means: For 5-year means, the RMSE was reduced by 38% (a 61% reduction in *E*), from 0.106°C to

Supporting Online Material material

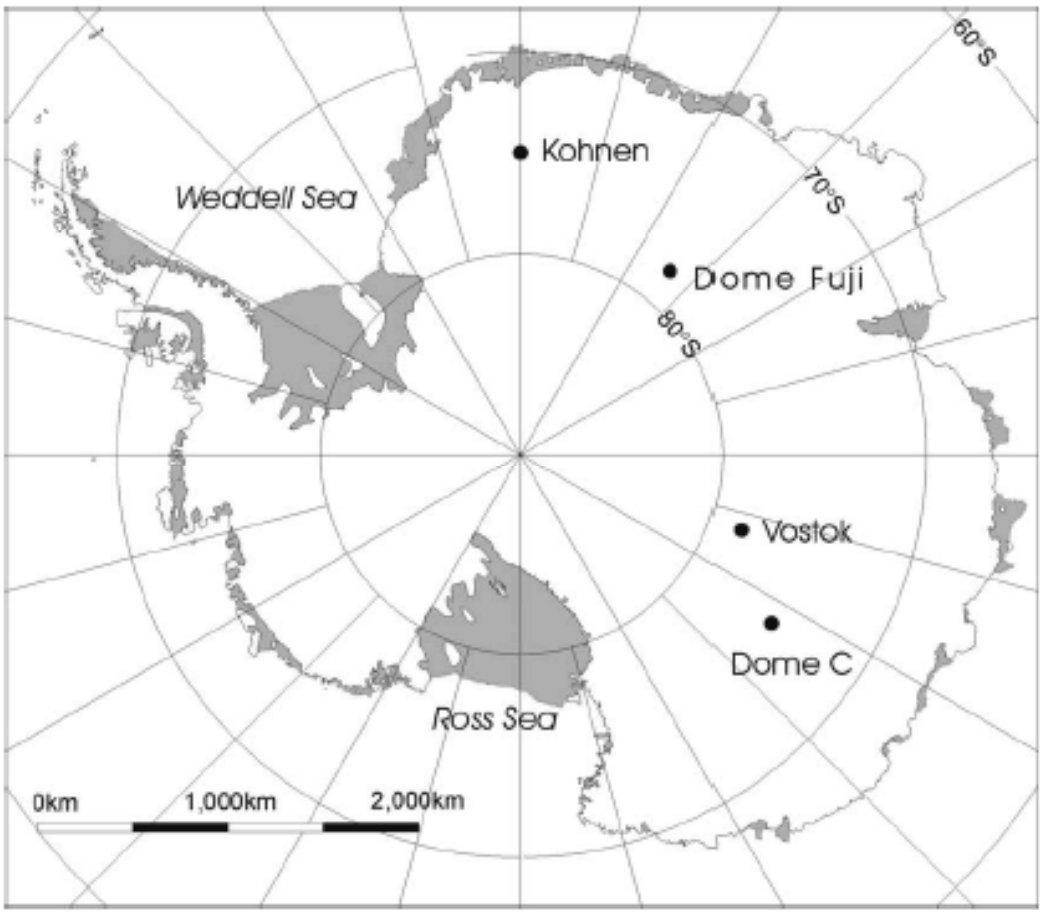

Figure S1 *: Map of deep ice core drillings in East Antarctica*

Drilling : At EPICA Dome C (75° 06' S, 123° 21' E), a depth of 3201 m was reached in January 2003. However, due to relatively warm ice (- 4 °C at 3201m), the drilling team faced difficulties at the end of the field season. Basal temperature is close to the melting point, a situation somewhat similar to that encountered at the Greenland North GRIP site (*1*). The Dome C drilling - postponed for one season - resumed in November 2004. In order to prevent melting and refreezing of drill chips in the hole and the drill from getting stuck, an ethanol water solution was added at the bottom of the drill hole. This method which had proven successful at North GRIP (*1*), allowed a final depth of 3260 m to be reached the following month. Drilling was stopped ~ 15 m above the bedrock to prevent

contamination of basal melt water by the drilling fluid (seismic soundings have suggested the presence of melt water just above the bedrock).

The deuterium profile : We have completed the deuterium measurements, δD_{ice}, with an optimal accuracy of ± 0.5 ‰ (1 σ), from the surface down to 3259.7 m, on a continuous and detailed basis of 55 cm along the entire core. Data are available at PANGEA and NCDC data centers.

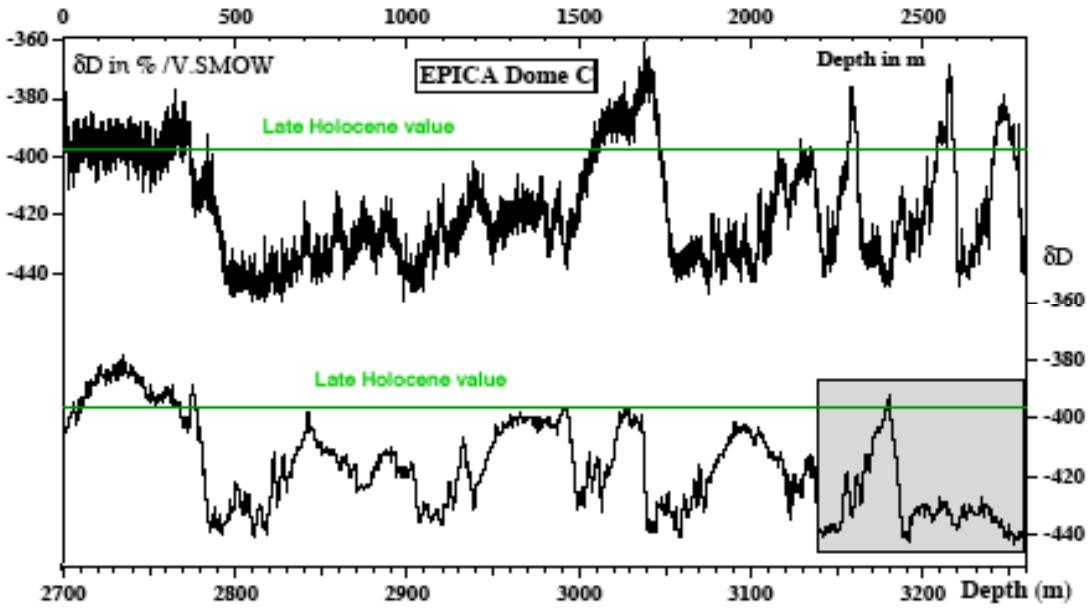

Figure S2 : *The 55 cm deuterium record as a function of depth in two parts. The extension of the record is highlighted by the grey rectangle. The horizontal lines correspond to the average deuterium value over the last 1000 years (late Holocene).*

The EDC3 timescale *:* This improved timescale is constructed in two steps (*2*, *3*). First (*2*), the same inverse modeling strategy as for EDC2 (*4*) is used, employing a glaciological dating model which combines an accumulation model and an ice flow model (*5*) constrained with chronological age markers. Additional time markers used for EDC3 include information derived from air content, which exhibits strong orbital

frequencies (6) and the Matuyama-Brunhes geomagnetic reversal (~ 780 ky BP) as recently identified between 3161 and 3170 m from beryllium 10 measurements (7). In a second step, flow anomalies, resulting in irregularities in the ice thinning function below ~ 2800 m, are accounted for using the precession driven $\delta^{18}O_{air}$ record available between 400 and 800 ky BP to tune this part of the chronology (3). Other notable improvements concern Termination II that was too young in EDC2 (*4*) and the last 40 ky over which the Antarctic (EDC and EDML) and Greenland ice records are now placed on a common timescale (*8, 9, 10*) .

The bottom part of the record : Figure S3 (left part) shows the new part of the record as a function of depth with corresponding ages indicated on the upper axis using the EDC3 timescale. If undisturbed, this part would cover MIS 20, 21 and 22, but while the oceanic record shows similar amplitudes for MIS 19 and 21, the δD_{ice} amplitude is three times smaller in this deepest part of the record than just above (Fig.S3). Oxygen 18 measurements performed on this bottom ice show the same low variability. Furthermore, the deuterium-excess profile is very flat and in the range of observed values in shallower ice, which rules out contamination of the ice by the ethanol added to the drilling fluid in the bottom part. Melting and refreezing of the ice can also be dismissed as the air content of the ice is comparable to shallower values. This leads us to suspect that the bottom 60 m of ice have been affected by flow disturbances, a situation previously encountered in Vostok ice below 3310 m (*11, 12*).

Indeed this lower than expected signal variability is shared by other parameters as illustrated in Fig.S3 by the oxygen 18 of O_2 in air ($\delta^{18}O_{air}$). This parameter depends on continental ice volume, and has been shown to vary coherently with precession over the last four climatic cycles with an amplitude of ~1 ‰ (*11, 13*). The very low amplitude of $\delta^{18}O_{air}$ before 800 ky BP (~ 0.2 ‰) despite precessional variability and significant

changes in ice-volume (*14*) argues strongly for the role of a flow disturbance. The same feature is observed for preliminary dust, CH_4 and CO_2 data (not shown). Our suspicion of flow disturbances is also supported by the presence of large particle inclusions. Whether these disturbances are due to stretching of this ice sequence or mixing of layers of different origins will be examined when high-resolution multiparametric records are available.

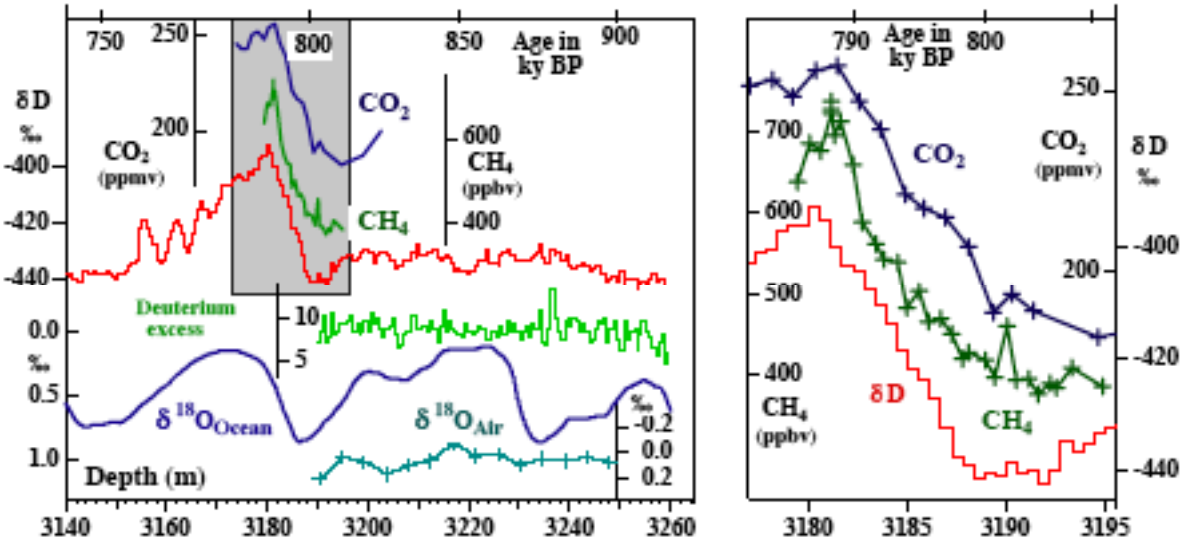

Figure S3 : *The left part of this graph shows the new part of the record as a function of depth with corresponding ages indicated on the upper axis using the EDC3 timescale. The ice below 3200 m is disturbed and cannot be interpreted climatically (although we still present the hypothetical ages from EDC3). For comparison, the ice sheet $\delta^{18}O$ contribution to the deep-sea core record is given as derived by Bintanja et al. (14), plotted against the EDC3 age scale (see upper axis). Additional data include the deuterium excess record ($\delta^{18}O$ measured at Copenhagen) and the $\delta^{18}O$ in air (measured in Saclay) for depths below 3200 m (older than 827 ky BP), as well as the CO_2 and CH_4 data measured along the transition from MIS 20 to MIS 19 (depth scale). The right part of the graph shows an expanded view of these CO_2 and CH_4 data illustrating the expected depth shifts between these measurements and the ice deuterium record.*

In contrast, the stratigraphic continuity of the record above ~3200 m is supported by all available data, especially by preliminary CO_2 and CH_4 measurements performed along the transition between MIS 20.2 and 19 (Fig. S3). In an undisturbed ice record, the changes in atmospheric CO_2 and CH_4 that accompany glacial-interglacial shifts must occur deeper in the ice than the deuterium signature of the temperature change. This is a necessary result of the gas enclosure processes that take place approximately 100 meters below the surface of the ice sheet (*15*). In contrast, the signatures of a disturbed stratigraphy are abrupt changes in both the deuterium and gas records at the same depth level, as observed in the Vostok ice (*11, 12*). No such anomaly has been detected at Dome C back to 650 ky BP (*16, 17*). The CO_2 and CH_4 data obtained on the transition between MIS 20.2 and 19 (Fig.S3) indicate a systematic shift in depth of at least 0.8 m with respect to the deuterium record at the end of the transition (corresponding to the peaks of MIS 19) and suggest a similar or larger shift at the start of the warming corresponding to the end of MIS 20.2. This precludes a depth reversal in the stratigraphic order of the layers. While awaiting the completion of gas measurements above this level, we provisionally assume that this holds true for the entire Dome C record back to MIS 20.2 and that the Dome C core provides a ~ 800 ky old reliable climatic record. As fully discussed by Dreyfus et al. (*3*), we have however indications from $\delta^{18}O_{air}$ measurements that ice thinning is not regular but with no compromise of the stratigraphy for ice between 800 m (MIS 12) and 3200 m (MIS 20.2), e.g. for the oldest 350 ky of the climatic record.

Isotopic modeling : Based on results inferred from simple Rayleigh type models, from existing simulations performed with atmospheric General Circulation Models implemented with water isotopes (IGCM), and from constraints on ice core chronologies and on gas age-ice age difference, it was concluded that at sites such as Vostok and EPICA Dome C, temperature changes are within - 10 % to + 30% of those obtained from

using the spatial δD/temperature slope (*18*). This result was independently supported by comparison between Byrd and Vostok data (*19*).

While the above-mentioned IGCM approaches only dealt with two different climates (*20, 21*), present-day and LGM, numerous time slices (present-day, pre-industrial, 6, 11, 14, 16, LGM and 175 ky BP) are considered for the ECHAM (22) simulations used for deriving the results presented in Figure S4, with corresponding boundary conditions extrapolated from CLIMAP data (*23*). In the Dome C sector (from the site to coastal Antarctica), the spatial gradients of all time slice calculations are remarkably constant varying by less than ±0.5‰/°C. The isotopes follow nearly exactly a Rayleigh distillation line in a wide temperature range between roughly –20°C to –70°C with isotopic values falling in a very small range for a given temperature, even under very different climate conditions.

This comprehensive modeling approach permits a direct comparison of the spatial slope in a given area with the temporal slope at a given site, allowing us to examine the validity of the isotopic paleothermometer (*24*). Figure S4 shows the mean isotope (δD) and surface temperature, T_s, in the Dome C model grid region plotted against each other. This temporal slope is not only very well defined ($r^2 = 0.94$) but its value (6.2 ‰/°C) is close to its modern spatial analogue of 6.04 ‰/°C (25). This good agreement between spatial and temporal slopes predicted for Dome C fully justifies the conventional temperature interpretation used here and we note that this IGCM modeling approach accounts for changes in origin and seasonality of precipitation. Indeed, the conventional approach leads to amplitudes quite similar to those obtained after correction for changes in source conditions from co-isotopic δD_{ice} and $\delta^{18}O_{ice}$ determinations performed on our Dome C core over the last 45 ky (*26 and therein*).

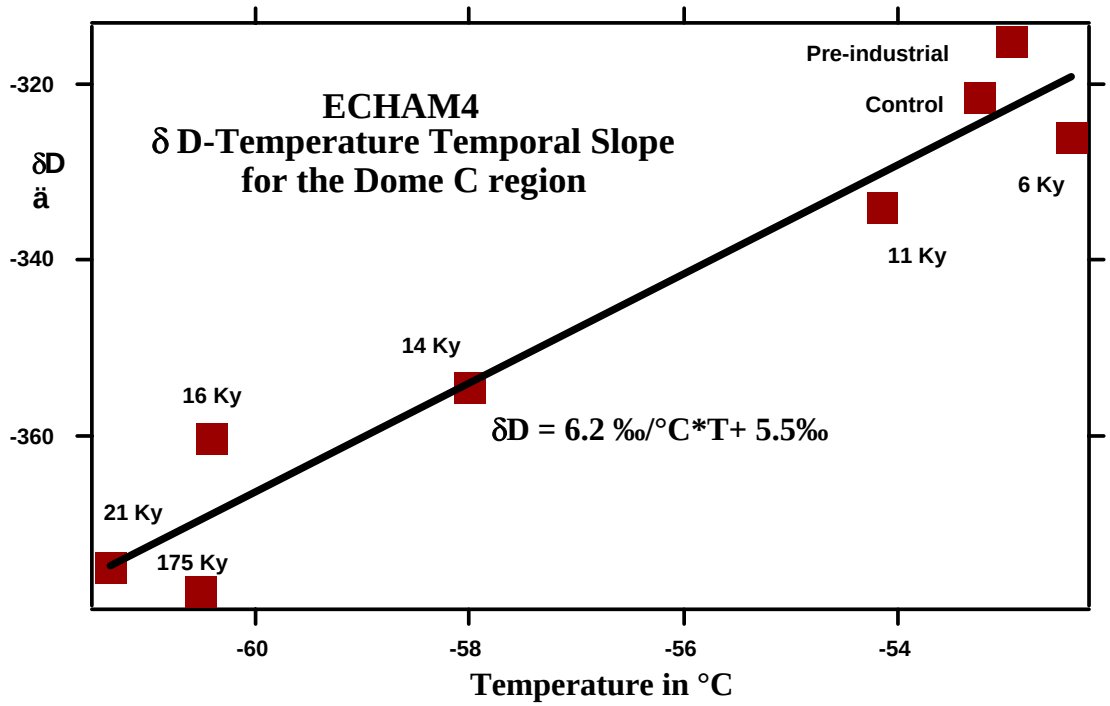

Figure S4 : *Results obtained from a series of new simulations performed using the isotopic version of the ECHAM General Circulation Model. Each square gives the corresponding δD (in ‰ wrt SMOW) and T_s values for the area corresponding to the Dome C site, with the best fit between these points providing the temporal slope.*

The surface temperature change, ΔT_s (estimated with respect to the mean value calculated over the last millenium), are calculated using the present-day spatial slope of 6.04 ‰/°C after correction for the change in the isotopic composition of the ocean (*13*) . We thus do not account at this stage of a temperature correction which would result for the change in the source temperature as estimated from co-istopic deuterium and oxygen 18 data (*26*) which are not yet available for the entire profile. We have also accounted for a slight correction linked with changes in the altitude of the ice sheet as calculated from the glaciological model used to derive the timescale. Typically the elevation decreases by

up to ~ 100 m for the coldest glacial periods with a corresponding temperature correction of ~ 1°C.

Millennial events : The timing between EDC and either North GRIP (Fig. 2) or EDML (Fig. S5) is established using the new common timescale developed for Greenland and Antarctic records. Synchronization between EDC and EDML uses volcanic events, with matching better than 1000 yr back to MIS 5.5 (8), while synchronization between EDML and North GRIP back to 52 ky BP is based on their CH_4 records with estimated uncertainties of ± 400 to ± 800 years largely linked to the gas age / ice age difference (8). In addition, the very detailed ^{10}Be measurements performed around the peak of production of this cosmogenic isotope (~ 40 ky BP) offers the opportunity for a direct and precise (± 200 yr) correlation between Dome C and Greenland records around this event which straddles AIM 10 (*27*). The temperature changes associated with these millennial Antarctic glacial events have been evaluated after detrending illustrating the succession of large AIM ("A" type event counterparts to long DO events often associated with Heinrich layers) and of smaller AIM that correspond to shorter DO events.

Figure S5 compares the EDC millennial variability with the corresponding variability at EDML (8) during the last glacial period, and at EDC for previous ones. The EDC record exhibits quite similar millennial climate variability during the last 3 glacial periods (Fig. S5) with σ of 0.65 and 0.55 °C during the penultimate and the third glacial periods. We confirm, in particular, the similarity between MIS 3 and MIS 8, previously discussed with the less detailed Vostok δD record (*28*). The σ value essentially depends on the succession of large AIM, but one can see from Fig. S5 that small AIM are easily identified back to MIS 10. The variability is lower during the previous glacial (σ = 0.43 °C for MIS 10) but still high during MIS 12 and MIS 14 (σ of 0.57 °C and 0.55 °C), only slightly lower for MIS 16 (σ of 0.48 °C) and again high for MIS 18 (σ of 0.64 °C).

However, smaller AIM are in any case more difficult to identify during MIS 12, 14, 16 and 18 as a result of lower resolution (one sample from these periods covers 400 to 700 yr). More detailed measurements are required to fully document the millennial variability before Termination V. Available samples will allow the resolution to be improved by a factor of 5.

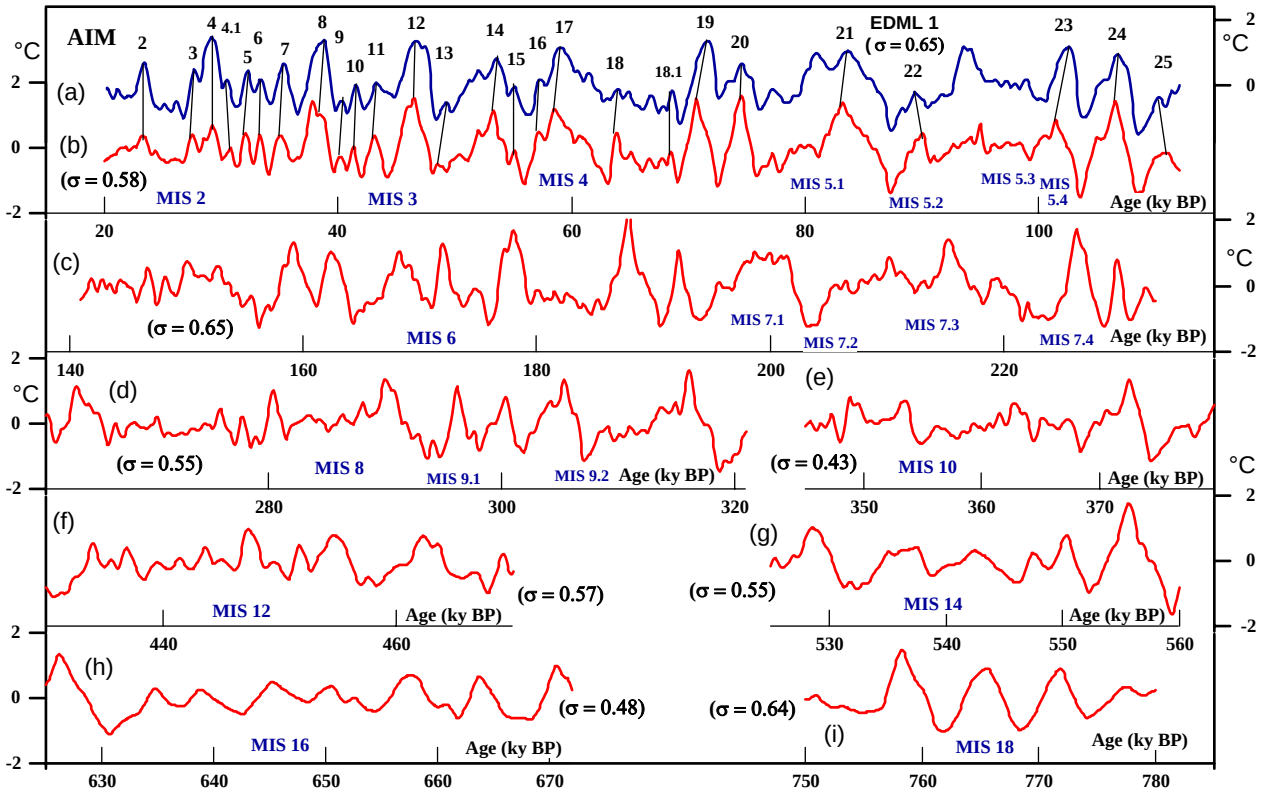

Figure S5 : *This graph compares the temperature variability at EDML (curve a) and EDC (curve b) during the last glacial period. Temperature reconstructions have been resampled on a 100 year time step and detrended. We show here the high frequency variability calculated using a 7-point Gaussian filter after detrending. Curves (c) to (i) show the millennial temperature variability at EDC calculated for previous glacial periods using the same algorithm.*

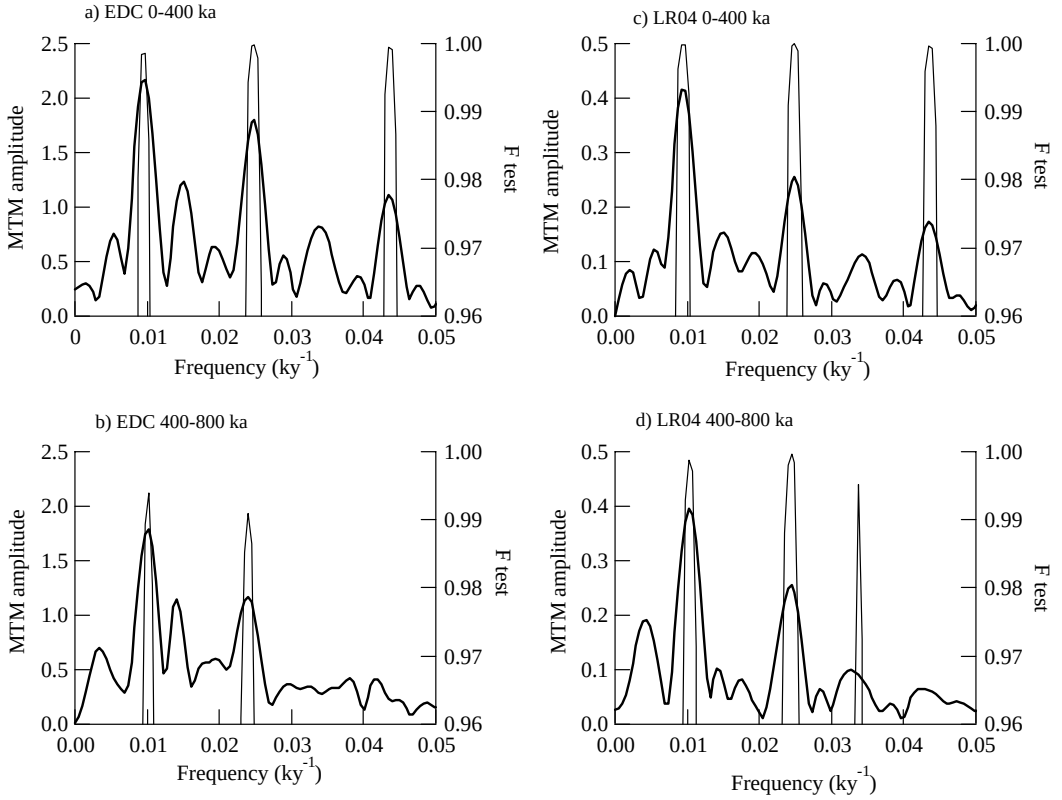

Figure S6 : *The power spectra of the ΔT_s EDC time series (left) and the Lisiecki and Raymo (25) stacked benthic oxygen 18 record (right) for two time periods : from 0 to 400 ky BP (top) and from 400 to 800 ky BP (bottom). In contrast to the Dome C record, the deep-sea core record has similar relative strength in the obliquity band for the two successive 400 ky periods, the deep-sea core record showing an increase in the amplitude of the obliquity component but only when considering longer time periods (29). These amplitude (continuous curve) and the associated statistical F-test (thin line) have been calculated with the Multi-Taper Method using the Analyseries software (30).*

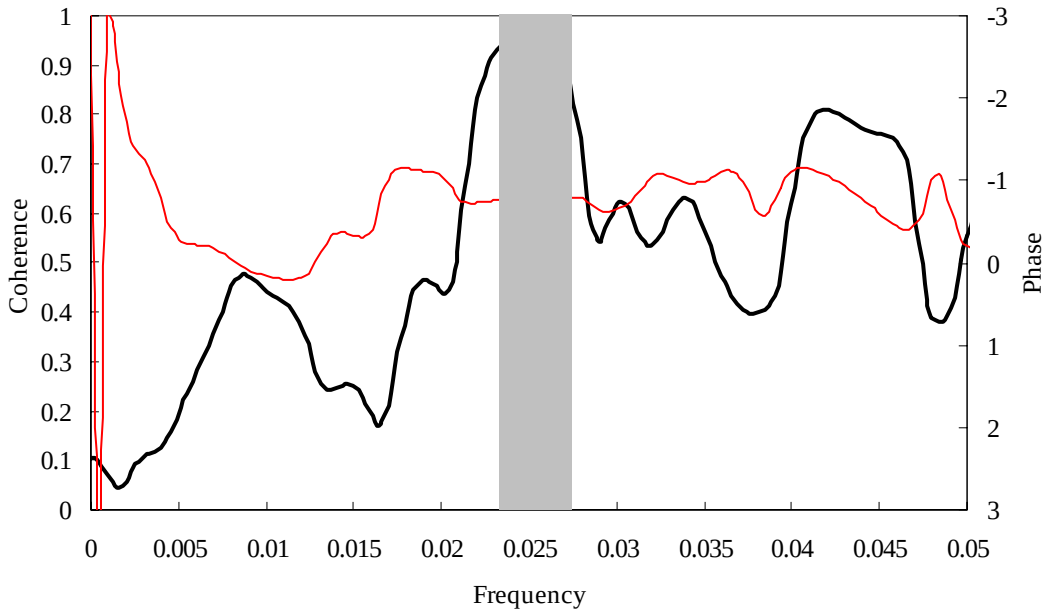

Figure S7 : *Analysis of coherence and phase between EDC temperature and 65°N mid-June insolation performed with the Analyseries software (30): coherence (black, left axis) and lag (radian, red, right axis) versus frequency (in ky^{-1}). The maximum coherence (0.97) is obtained in the obliquity range (grey shaded area) and corresponds to a 5 ky lag of temperature with respect to obliquity. Similar results are obtained when considering the first and second parts of the records (0-400 and 400-800 ka) and when considering obliquity instead of 65°N mid-June insolation.*

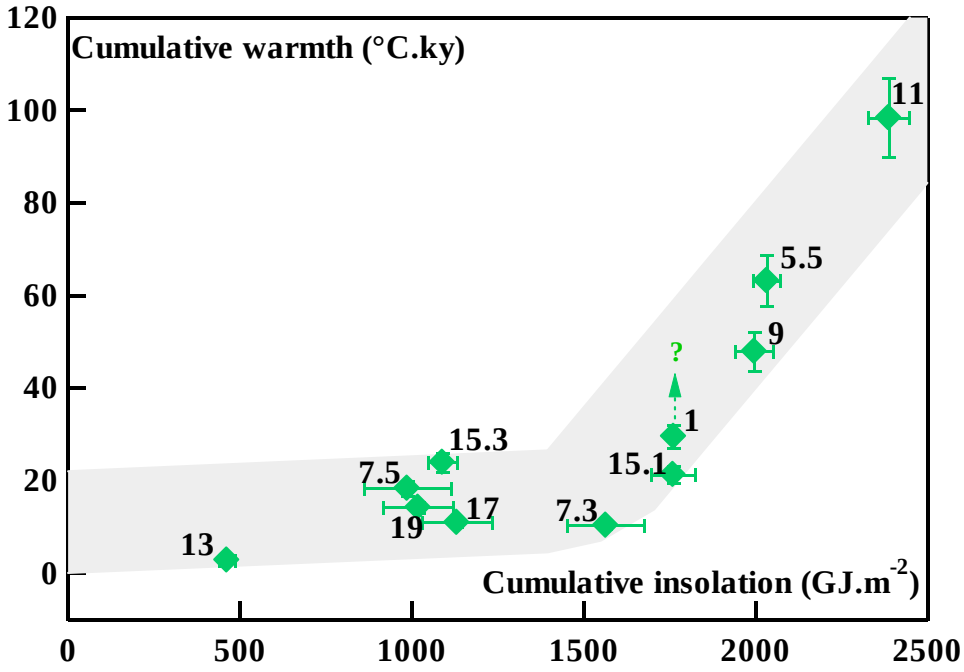

Figure S8 : *Cumulative warmth (°C.ky) calculated as the integral of Dome C temperature reconstruction above a threshold of -2.5°C (indicated by the horizontal dashed line on Figure 3), represented against cumulative insolation (GJ.m^{-2}), calculated from positive anomalies of centered 60°S annual mean insolation shifted by 5 kyr. Because the current interglacial period, MIS 1, is still ongoing, a vertical dashed arrow indicates the expected direction for MIS 1 total cumulative warmth.*

References

1. North Greenland Ice-core project (NorthGRIP), *Nature*, **431**, 147 (2004).

2. F.Parennin et al, *Climate of the Past Discussions*, **3**, 19 (2007).

3. G.Dreyfus et al., *Climate of the Past Discussions*, **3**, 63 (2007).

4. EPICA Community members, *Nature*, **429**, 623 (2004).

5. F.Parrenin, J.Jouzel, C.Waelbroeck, C.Ritz and J.M.Barnola, *J. Geophys. Res.*, **106**, 31837 (2001).

6. Raynaud, D. et al., Earth Planet Sci. Lett., submitted.

7. G.M.Raisbeck, F.Yiou, O.Cattani & J.Jouzel, *Nature*, **444**, 82 (2006).

8. EPICA Community members, *Nature*, 195, 444 (2006).

9. S.O.Rasmussen et al., *J.Geophys.Res*, **111**, doi:10.1029/2005JD006079 (2006).

10. K.K.Andersen et al., *Quat.Sci.Rev*., submitted (2006).

11. J.R. Petit et al. *Nature*, **399**, 429 (1999).

12. D.Raynaud et al. *Nature*, **436,** 39 (2005).

13. M.Bender, Earth Planet Sci. Lett.,, 204, 275-289 (2002).

14. R.Bintanja, R.S.W van de Wal, R.S.W. & J.Oerlemans, *Nature*, **437**, 125 (2005).

15. J.M.Barnola, P.Pimienta, D.Raynaud & Y.S.Korotkevich, *Tellus*, **43B**, 83 (1991).

16. U.Siegenthaler et al., *Science*, **310**, 1313 (2005).

17. R.Spahni et al., *Science*, **310**, 1317 (2005).

18. J.Jouzel et al., *J.Geophys.Res.*, **108**, doi: 10.1029/2002JD002677 (2003).

19. T.Blunier, J.Schwander, J. Chappellaz, F.Parrenin & J.M.Barnola, *Earth Planet. Sci. Lett.*, **218**, 379 (2004).

20. J.Jouzel, R.D.Koster, R.J.Suozzo & G.L.Russell, *J.Geophys.Res.*, 99, D12, 25791 - 25801, 1994.

21. J.Jouzel, G.Hoffmann, R.Koster & V.Masson, *Quat.Sci.Rev*., **19**, 363 (2000).

22. G.Hoffmann, M. Werner & M.Heimann, *J.Geophys.Res.*, **103**, 16871, 1998.

23. CLIMAP. *Seasonal reconstructions of the Earth's surface at the last glacial maximum* (Geol. Soc. Am., Boulder, CO, 1981).

24. J.Jouzel et al., *Nature*, **329**, 402(1987).

25. C.Lorius & L.Merlivat in *Isotopes and impurities in snow and ice. Proceedings of the Grenoble Symposium Aug./Sep. 1975* (ed. IAHS) 125, IAHS, Vienna (1977).

26. B.Stenni et al., *Earth Planet. Sci. Lett.*, **217**, 183 (2004).

27. G.M.Raisbeck, F.Yiou, F.& J.Jouzel, *GCA*, **66**, A623 (2002).

28. M.Siddall, T.F. Stocker, T. Blunier, R. Spahni, J.-M. Barnola, and J. Chappellaz, *Paleoceanography*, in press (2006).

29. L.E.Lisiecki & M.E. Raymo, *Paleoceanogr.*, **20,** doi:10.1029/2004PA001071 (2005).

30. D.Paillard, L.Labeyrie & P.Yiou, *EOS, Trans. AGU*, **77**, 379 (1996).